Year: 2023

# Load distribution on intervertebral cages with and without posterior instrumentation

Calek, Anna-Katharina ; Cornaz, Frédéric ; Suter, Mauro ; Fasser, Marie-Rosa ; Baumgartner, Sina ; Sager, Philipp ; Farshad, Mazda ; Widmer, Jonas

Abstract: BACKGROUND CONTEXT Posterior and transforaminal lumbar interbody fusion (PLIF, TLIF) are well-established procedures for spinal fusion. However, little is known about load sharing between cage, dorsal construct, and biological tissue within the instrumented lumbar spine. PURPOSE The aim of this study was to quantify the forces acting on cages under axial compression force with and without posterior instrumentation. STUDY DESIGN Biomechanical cadaveric study. METHODS Ten lumbar spinal segments were tested under uni-axial compression using load cell instrumented intervertebral cages. The force was increased in 100N increments to 1000N or a force greater than 500N on one load cell. Each specimen was tested after unilateral PLIF (uPLIF), bilateral PLIF (bPLIF) and TLIF each with/without posterior instrumentation. Dorsal instrumentation was performed with 55N of compression per side. RESULTS Cage insertion resulted in median cage preloads of 16N, 29N and 35N for uPLIF, bPLIF, and TLIF. The addition of compressed dorsal instrumentation increased the median preload to 224N, 328N, and 317N, respectively. With posterior instrumentation, the percentage of the external load acting on the intervertebral cage was less than 25% at 100N (uPLIF: 14.2%; bPLIF: 16%; TLIF: 11%), less than 45% at 500N (uPLIF: 31.8%; bPLIF: 41.1%; TLIF: 37.9%) and less than 50% at 1000N (uPLIF: 40.3%; bPLIF: 49.7%; TLIF: 43.4%). Without posterior instrumentation, the percentage of external load on the cages was significantly higher with values above 50% at 100N (uPLIF: 55.6%; bPLIF: 75.5%; TLIF: 66.8%), 500N (uPLIF: 71.7%; bPLIF: 79.2%; TLIF: 65.4%), and 1000N external load (uPLIF: 73%; bPLIF: 80.5%; TLIF: 66.1%). For absolute loads, preloads and external loads must be added together. CONCLUSIONS Without posterior instrumentation, the intervertebral cages absorb more than 50% of the axial load and the load distribution is largely independent of the loading amplitude. With posterior instrumentation, the external load acting on the cages is significantly lower and the load distribution becomes load amplitude dependent, with a higher proportion of the load transferred by the cages at high loads. The bPLIF cages tend to absorb more force than the other two cage configurations. CLINICAL SIGNIFICANCE Cage instrumentation allows some of the compression force to be transmitted through the cage to the screws below, better distributing and reducing the overall force on the pedicle screws at the end of the construct and on the rods.

Basic science

# Load distribution on intervertebral cages with and without posterior instrumentation

Anna-Katharina Calek, MD[a,*], Frédéric Cornaz, MD[a], Mauro Suter[c],
Marie-Rosa Fasser, MSc[c], Sina Baumgartner, BSc[c], Philipp Sager, MD[c],
Mazda Farshad, MD, MPH[a,b], Jonas Widmer, PhD[c]

[a] *Department of Orthopedics, Balgrist University Hospital, University of Zurich, Forchstrasse 340, Zurich CH-8008, Switzerland*
[b] *University Spine Center Zurich, Balgrist University Hospital, University of Zurich, Zurich, Switzerland*
[c] *Spine Biomechanics, Department of Orthopedic Surgery, Balgrist University Hospital, University of Zurich, Zurich, Switzerland*

Abstract

**BACKGROUND CONTEXT:** Posterior and transforaminal lumbar interbody fusion (PLIF, TLIF) are well-established procedures for spinal fusion. However, little is known about load sharing between cage, dorsal construct, and biological tissue within the instrumented lumbar spine.

**PURPOSE:** The aim of this study was to quantify the forces acting on cages under axial compression force with and without posterior instrumentation.

**STUDY DESIGN:** Biomechanical cadaveric study.

**METHODS:** Ten lumbar spinal segments were tested under uniaxial compression using load cell instrumented intervertebral cages. The force was increased in 100N increments to 1000N or a force greater than 500N on one load cell. Each specimen was tested after unilateral PLIF (uPLIF), bilateral PLIF (bPLIF) and TLIF each with/without posterior instrumentation. Dorsal instrumentation was performed with 55N of compression per side.

**RESULTS:** Cage insertion resulted in median cage preloads of 16N, 29N and 35N for uPLIF, bPLIF, and TLIF. The addition of compressed dorsal instrumentation increased the median preload to 224N, 328N, and 317N, respectively. With posterior instrumentation, the percentage of the external load acting on the intervertebral cage was less than 25% at 100N (uPLIF: 14.2%; bPLIF: 16%; TLIF: 11%), less than 45% at 500N (uPLIF: 31.8%; bPLIF: 41.1%; TLIF: 37.9%) and less than 50% at 1000N (uPLIF: 40.3%; bPLIF: 49.7%; TLIF: 43.4%). Without posterior instrumentation, the percentage of external load on the cages was significantly higher with values above 50% at 100N (uPLIF: 55.6%; bPLIF: 75.5%; TLIF: 66.8%), 500N (uPLIF: 71.7%; bPLIF: 79.2%; TLIF: 65.4%), and 1000N external load (uPLIF: 73%; bPLIF: 80.5%; TLIF: 66.1%). For absolute loads, preloads and external loads must be added together.

**CONCLUSIONS:** Without posterior instrumentation, the intervertebral cages absorb more than 50% of the axial load and the load distribution is largely independent of the loading amplitude. With posterior instrumentation, the external load acting on the cages is significantly lower and the load distribution becomes load amplitude dependent, with a higher proportion of the load transferred by the cages at high loads. The bPLIF cages tend to absorb more force than the other two cage configurations.

---

*Corresponding author. Department of Orthopedics, Balgrist University Hospital, University of Zurich, Forchstrasse 340, Zurich CH-8008, Switzerland Tel.: +41 44 386 11 11.

*E-mail addresses:* spine@balgrist.ch (A.-K. Calek), jonas.widmer@balgrist.ch (J. Widmer).

**CLINICAL SIGNIFICANCE:** Cage instrumentation allows some of the compression force to be transmitted through the cage to the screws below, better distributing and reducing the overall force on the pedicle screws at the end of the construct and on the rods.   © 2023 The Author(s). Published by Elsevier Inc. This is an open access article under the CC BY license (http://creativecommons.org/licenses/by/4.0/)

## Introduction

Lumbar interbody fusion is a well-established surgical procedure for the treatment of degenerative conditions of the lumbar spine. Posterior and transforaminal lumbar interbody fusion (PLIF, TLIF) are the most commonly used [1,2] and provide the ability for solid fusion in the intervertebral space with direct neural decompression, historically higher fusion rate than bone graft alone [3], restoration of intervertebral height, and assistance in restoring sagittal and coronal alignment [4,5].

The use of intervertebral cages in spinal fusion has three main advantages: First, they have a biological purpose: bone grafts can be inserted into the intervertebral space, improving and accelerating fusion [6]. Second, the intervertebral space can be expanded by inserting a cage, and thus a higher degree of lordosis can be achieved by dorsal compression using the hypomochlion created by the cage [7]. The third and probably least considered advantage is biomechanical: the rigid cage reduces the elasticity of the disc space and thus stiffens the ventral column. As a result, more of the vertical compressive forces can be transferred away from the dorsal instrumentation to the ventral column of the spine [8]. Relieving the dorsal instrumentation from biomechanical loads, which could reduce the risk of implant failure as well as screw loosening, which is one of the major complications of fusion surgery. Of course, this effect is only significant in the early postoperative period, when bony fusion has not yet been achieved. This hypothesized biomechanical mechanism is further discussed and illustrated in the discussion section of this manuscript (Fig. 7).

To assess the relevance of this effect, knowledge of the load acting on the cage is essential. Axial compressive loads in the lumbar spine are in the range of 1000N in an upright position, such as standing, and increase to more than 3000N during daily activities [9,10]. A number of studies have investigated the different cage designs and their positioning in the intervertebral space [5,9,11]. However, there is a lack of biomechanical studies that demonstrate the actual force applied to the cages. Du et al. [12] conducted a study in this regard, but it had several limitations: the axial compression force applied to the vertebral segments was limited to 400N; furthermore, the cage loading ratio was reported without the corresponding preload; and a simplified test cage was used with only one load cell in combination with an axial guide, which could have absorbed some of the applied loads.

Therefore, the aim of this biomechanical study was to quantify the force acting on cages under different amplitudes of axial compression with and without posterior instrumentation and with three different cage configurations: unilateral PLIF (uPLIF), bilateral PLIF (bPLIF), and TLIF. This information was further used to compute the load distribution between cage, posterior instrumentation, and biological tissue.

## Materials and methods

### Dissection, preparation, and storage

The study was approved by the responsible investigational review board. Ten spinal segments (one L1/2, two L2/3, three L3/4, three L4/5, and one L5/S1) originating from six fresh frozen cadavers (Science Care, Phoenix, AZ, USA) with a mean age of 55.4 years (range 36−75, two males and three females) were tested. Specimens were stored at −20°C until further dissection and biomechanical testing. Computed tomography (CT) scans (SOMATOM Edge Plus, Siemens Healthcare GmbH, Erlangen, Germany) were performed to exclude bony defects. The specimens were thawed overnight at a room temperature of 20°C and carefully dissected from the surrounding tissue without damaging the bony processes, the intervertebral disc and the spinal ligaments. After preparation, the segments were mounted on a testing machine using customized 3D-printed-clamps [13,14].

### Instrumentation of the spinal segments and cage insertion

Each spinal segment was instrumented with four pedicle screws with a screw diameter of 6 mm and length of 40 to 50 mm (Fig. 1A, 2A and B). After predrilling with a 2.7 mm drill bit, the screws (cannulated polyaxial titanium alloy pedicle screws, Medacta International, Castel San Pietro, Switzerland) were inserted. The spinous process of the cranial vertebra was partially removed, as well as the supraspinous and interspinous ligaments. To allow for the force measurement at the intervertebral cages, replica of commercially available 3D-printed titanium PLIF and TLIF cages were used. While the cages had the same outer dimensions as the original product, it was composed of a cranial and caudal piece with two load cells in between. Further details on the design, the load cells and the validation experiments can be found in Appendix 1. For uPLIF insertion, a unilateral laminotomy was performed to gain access to the intervertebral space. If required, a sparing medial partial facetectomy (25%−50%) was performed. For the bPLIF, the same procedure was performed on the opposite side. For TLIF insertion, a total facetectomy was performed ipsilateral to the cage insertion. The contralateral facet was
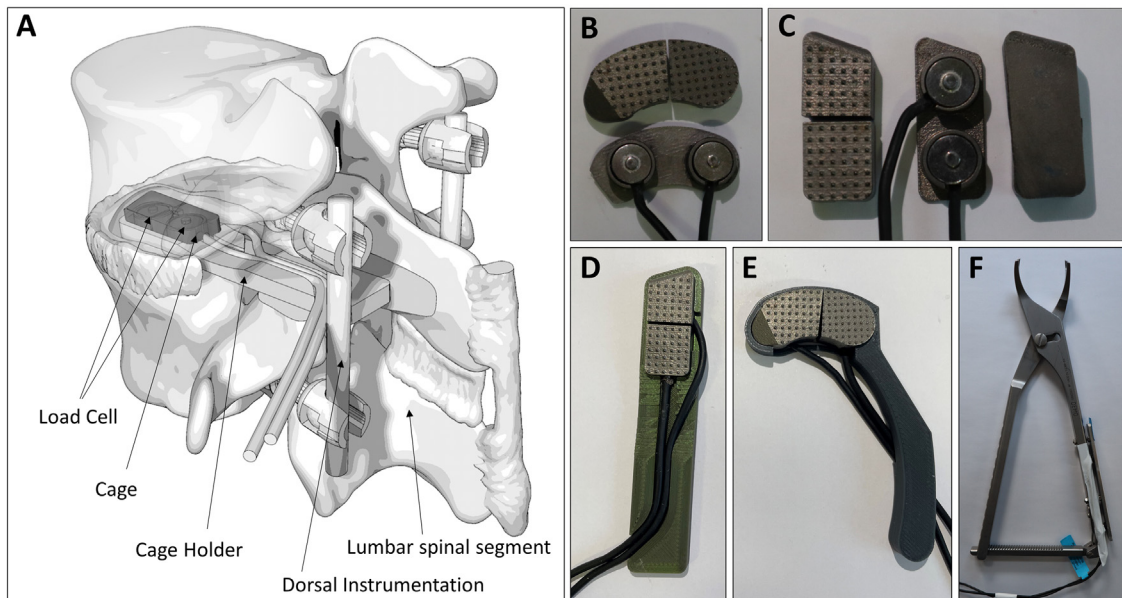
Fig. 1. lllustration of a lumbar segment following dorsal instrumentation and placement of a unilateral PLIF cage (A). TLIF cage (B) and PLIF cage (C) equipped with two load cells. PLIF and TLIF cage with corresponding insertion tool (D+E). Compression tongs equipped with two load cells to measure and standardize the applied compression force (F).

preserved. For each cage type, the disc space at the implantation site was cleaned with curettes and rongeurs, taking care not to damage the endplates. For the configuration with dorsal instrumentation (screw-rod-system), 5.5 mm titanium rods were attached to the two screw heads on each side, and the screw heads were sequentially compressed with a modified load cell-equipped compression tong (Medacta, M.U.S.T) (Fig. 1F) that allowed measurement of the applied force, which was set at 55N on each side. A total force of 110N was chosen because, prior to this study, all in-house spine surgeons were asked to apply compression to a posterior instrumentation model that they would use intraoperatively. The measured grip force was then converted to the compression force applied to the screw heads.

The compression force was measured and resulted in a mean of 116N. Therefore, a standardized force of 55N was applied to each rod for preload as measured with the compression tongs described above. This force was applied with a deviation of 10% and resulted in a compression force of approximately 224N (force = moment/distance (in meters) between the end of the jaw and the joint of the compression tongs: 16.77/0.075) at the rod site.

The absolute force (median, percentile) applied to the three different cage configurations with and without instrumentation is shown in Fig. 4.

The spinal segments were instrumented by a fellowship-trained orthopedic surgeon. Because isolated segments of the lumbar spine were instrumented, the
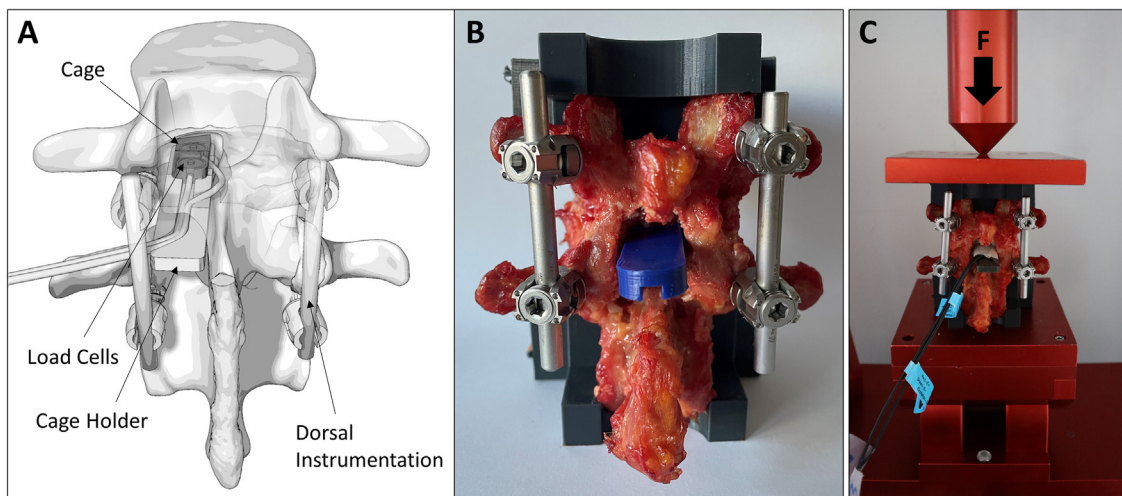


Fig. 2. Dorsal view of a lumbar segment after dorsal instrumentation and insertion of a unilateral PLIF cage (A); dorsal view after midline approach with a placeholder inserted to determine the required cage height (B). Biomechanical test setup for application of a vertical compression force (C).

correct position of the pedicle screws could be confirmed by visualization, as no medial or lateral penetration of the screws was visible.

*Biomechanical experiments and testing protocol*

Biomechanical testing was performed on a biaxial (linear and torsional) static testing machine (Zwick/ Roell Allroundline 10kN and testXpert III Software, ZwickRoell GmbH & Co. KG, Germany; Fig.1). Uniaxial compression load was applied to a point in the midline between the middle and dorsal third of the cranial endplate of the caudal vertebra, while the caudal vertebra was mounted on an x-y-stage (Fig. 2C).

Prior to teasting each configuration, the specimens were precycled with an axial compression of up to 1000N at 5 mm/min. Premature termination of precycling was required when the force in one of the load cells exceeded 500N (due to the acceptable limit of the load cells used). After release of the precycling load, the resting regime was performed, which consisted of a stepwise increase of axial compressive load from 0 to 1000N in increments of 100N. The load increase was performed at 5mm/min in accordance with the ASTM standard [15]. Each step was held for 8 seconds to allow for force stabilization prior to recording. Analogous to precycling, the test regime was stopped when the load on one of the load cells exceeded 500N. The test protocol was employed for the following configurations: uPLIF with posterior instrumentation, uPLIF without posterior instrumentation, bPLIF with posterior instrumentation, bPLIF without posterior instrumentation, TLIF with posterior instrumentation, and TLIF without posterior instrumentation.

## Data evaluation and statistical analysis

Data analysis was performed with MATLAB (Matlab 2020b, MathWorks, MA, USA). For all the load cell recordings, the measured forces were determined without external loading (preload) and after each load increment. Except for the evaluation of anterior-posterior load sharing, the measurements from the load cells (two for TLIF, two for uPLIF and four for bPLIF) were summed. The compressive force on the cage without external loading (preload) was assessed for uPLIF, bPLIF and TLIF with and without instrumentation. For each segment, a curve was fitted through all measurements in increments of 100N up to the maximum applied axial load. Since in certain cases, axial loading had to be stopped before reaching 1000N (to avoid overloading of the load cells), the dataset was incomplete. Of the ten specimens, complete data sets were obtained in eight (80%), nine (90%), and five (50%) for the dorsal rod configuration for uPLIF, bPLIF, and TLIF, respectively. Without posterior instrumentation, complete data sets were obtained for six (60%), 10 (100%), and seven (70%) specimens, respectively. To prevent bias associated with ignoring these missing data points (eg, situations with uneven load distribution or above-average cage loading), curve extrapolation

was performed to complete the data set: The measurements were completed by spline extrapolation of the difference between the average of the completed measurements and the partial recordings.

For each of the three cage configurations, the additional force on the cages due to external loading at 100N, 500N, and 1000N was compared between the posteriorly instrumented and the non-instrumented conditions. Furthermore, the measured load at 1000N was compared between TLIF, uPLIF and bPLIF in the condition with and without rod instrumentation. Paired nonparametric comparisons (Wilcoxon signed-rank test) were performed. The significance level $\alpha$ was set to 0.05 and the p-value was corrected according to Bonferroni.

Load sharing between the anterior and the posterior components of the PLIF cage(s) with posterior instrumentation was assessed at 0N (preload only) and 1000N external loading and can be found in Appendix 2. For this evaluation, only the complete datasets were considered. For bPLIF, the recorded forces from the left and the right load cells were summed.

If not otherwise specified, data are reported as median (25th percentile − 75th percentile).

Finally, load sharing between cage, tissue, and rod construct was estimated using the available measurements for each cage type. First, the load sharing between the cage and biological tissue was determined based on the results obtained without posterior instrumentation. We assumed that this ratio between cage loading and tissue loading would remain constant for a given measured load, regardless of the presence or absence of posterior rod instrumentation. The instrumented segment measurements were then used to estimate the load sharing between the three components for various external loads and the three cage types.

## Results

*Preload of the different cage configurations (uPLIF, bPLIF, TLIF) after cage insertion and posterior compression (110N)*

Without external loading, a median force of 16.4N (10.9 −38.3N) was measured on the uPLIF cage, which increased significantly (p=.04) to 223.8N (61.4−357.1N) after posterior instrumentation, using the standardized force of 55N through the compression tongs. On the bPLIF, a median force of 28.9N (22.7−38.8N) was measured after cage insertion, which increased significantly (p=.04) to 328.2N (227.3−469.3N) after posterior compression and instrumentation. On the TLIF cage, a median force of 35N (23.5 −81.5N) was measured, which increased significantly (p=.04) to 316.9N (119.3−370N) after posterior compression and instrumentation (Fig. 3).

*Percentage of external load acting on the uPLIF, bPLIF and TLIF cage with and without posterior instrumentation*

Of the ten specimens, complete datasets were acquired in eight, nine, and five for the configuration with dorsal rods
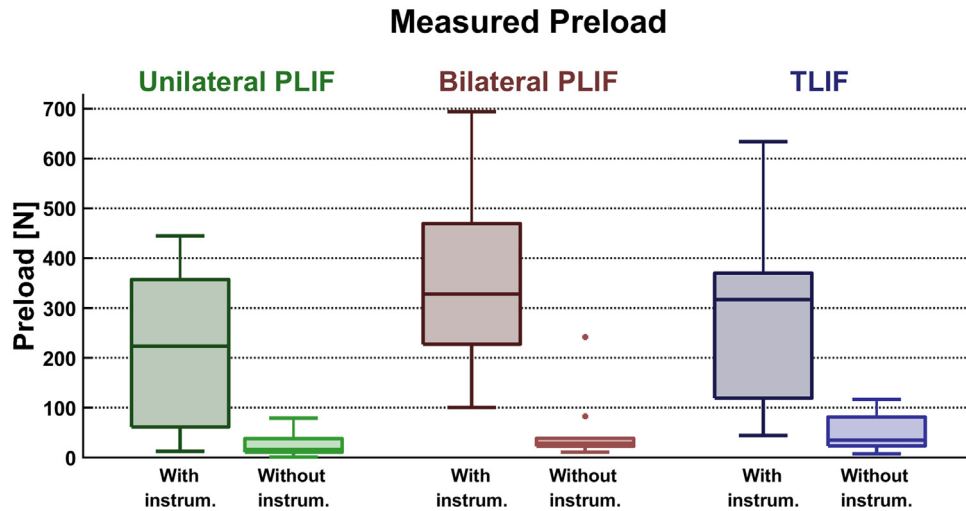
## Measured Preload



Fig. 3. Absolute preload (N) acting on three different cage configurations with and without instrumentation.

for uPLIF, bPLIF, and TLIF, respectively. For the configuration without dorsal rods, complete data sets were obtained for six, 10, and seven specimens, respectively. For the following analysis, the remaining datapoints were extrapolated as explained in the method section. To assess the percentage of the external load acting on the cage, the preload due to cage insertion and dorsal compression was subtracted. Detailed results including median and ranges can be found in Table 1 and the data are illustrated in Fig. 4.

With posterior instrumentation, the load on the cage was less than 25% at 100N load, less than 45% at 500N and less than 50% at 1000N. Without posterior instrumentation, the load on the intervertebral cages was significantly higher (p=.04 for all comparisons) with values above 50% at 100N, 500N, and 1000N external load. With posterior instrumentation at maximum axial compression (1000N), the cages showed comparable axial force absorption, although the bPLIF cages tended to absorb more force than the other two cage configurations (Fig. 4).

The values considered do not take into account the preload, only the effect of the external load was compared.

## Discussion

The most important finding of the present study is that in the configuration without posterior instrumentation, more than 50% of the externally applied compressive load is transferred by the intervertebral cages, a value that was largely independent of the loading amplitude. Although this configuration is not typically employed in the clinical routine, it illustrates the potential of the intervertebral cage as a propping structure. With the higher stiffness of the cage compared with the surrounding intervertebral disc, it absorbs most of the load and thus can reduce loading of the biological structures, which may help prevent further degeneration or specific problems such as herniation of the remaining disc material.

In the posterior instrumentation configuration, the proportion of external load acting on the cages was significantly smaller compared with the configuration without posterior instrumentation for all cage configurations and for all loading amplitudes. However, in this configuration, the proportion of external load acting on the cages was dependent on the loading amplitudes, with less than 25% of the external load acting on the cage at 100N external loading and almost 50% at 1000N. This observation leads to the intuitive conclusion that the addition of a posterior screw-rod-construct can relieve the cage of a portion of the external compressive loading, especially at low loading amplitudes.

However, this analysis focuses only on the force caused by external loading and does not include the compressive force caused by posterior compression of the screw-rod construct. The 55N compression on either side caused an increase in the compressive load on the cage of 200 to

Table 1
Median and percentiles of percentage of external loading for the three different cage configurations with and without posterior instrumentation (PI)

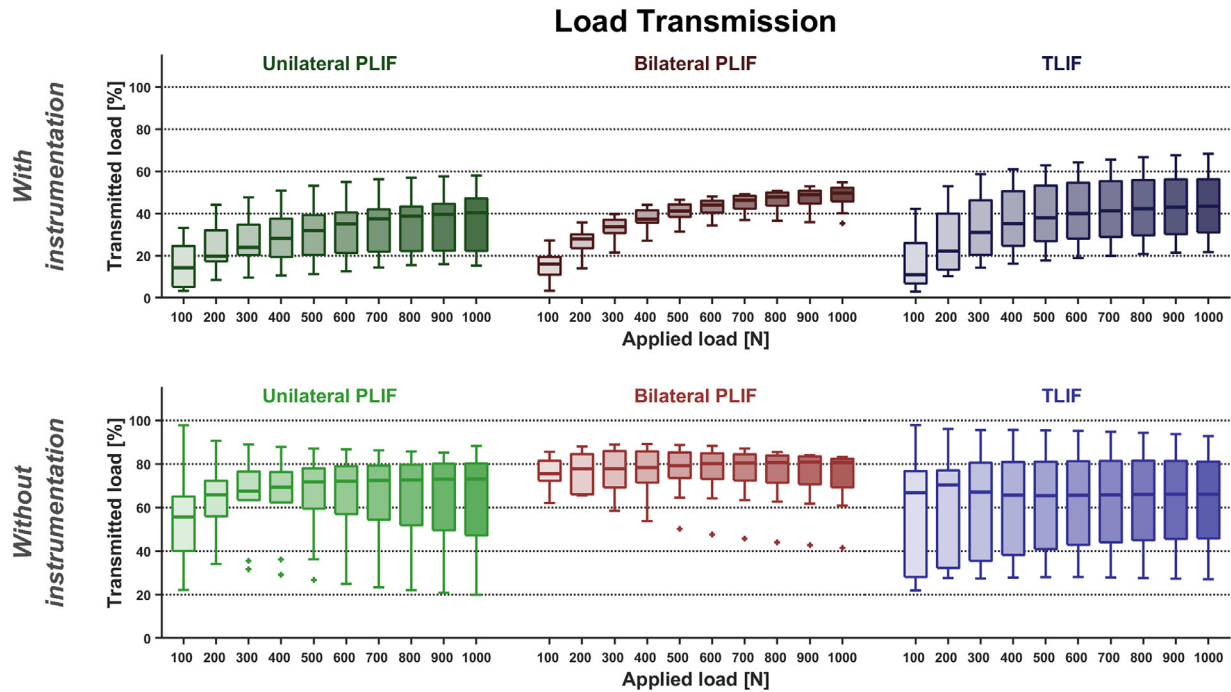| | Unilateral PLIF | | Bilateral PLIF | | TLIF | |
|---|---|---|---|---|---|---|
| | With PI | Without PI | With PI | Without PI | With PI | Without PI |
| **100 N** | 14.2% (5.1−24.5%) | 55.6% (40−65.1%) | 16% (10.9−19.3%) | 75.5% (72.3−81.5%) | 11% (6.7−25.9%) | 66.8% (28.1−76.7%) |
| **500 N** | 31.8% (20.3−39.2%) | 71.7% (59.4−78%) | 41.1% (38.4−44.3%) | 79.2% (73.6−85.3%) | 37.9% (26.8−53.2%) | 65.4% (40.9−81%) |
| **1000 N** | 40.3% (22.2−47.1%) | 73% (47.2−80.2%) | 49.7% (45.7−52.2%) | 80.5% (69.3−82.3%) | 43.4% (31−56.1%) | 66.1% (45.8−81.1%) |

**Load Transmission**



Fig. 4. illustrates the percentage of the externally applied force acting on the different cage configurations with and without posterior instrumentation (including extrapolated data). The externally applied force (x-axis) was increased in 100N increments and was counted as 100% for every datapoint.

300N, resulting in a significantly larger absolute load on the cage at 0N external loading for all cage configurations. Interestingly, at higher external loading, the difference between the configuration with and without posteriorly compressed screw-rod constructs became insignificant. This observation can be explained by the ability of the posterior-screw rod construct to absorb externally applied axial compressive force, which at higher loading amplitudes can even counteract the additional load caused by the posterior compression of the screw heads. One can assume that without posterior compression, the cage would be exposed to less axial compressive loading, while the screw-rod construct would bear more load. However, this load redistribution towards the posterior instrumentation would be unwanted, as in the clinical routine, posterior instrumentation failure (rod or screw breakage, screw loosening) is typically more common and more detrimental than ventral instrumentation failure (cage subsidence, cage failure). The biomechanical goal of cage insertion is (among others) to protect the posterior screw-rod construct, and posterior compression appears to be helpful for this purpose.

Another potential problem of posterior compression could be an uneven load distribution between the anterior and posterior part of the PLIF cages. While this disbalance was observed in the situation without external loading, a relevant redistribution of the load towards the anterior part of the PLIF cages was observed, which balanced the load distribution and reduced the risk of localized endplate overloading (Appendix 2).

Comparing the three different cage configurations, the bPLIF appears to be most appropriate, as this configuration

tended to absorb more force than the TLIF or the uPLIF cage. This observation can be explained by the larger contact surface of the bPLIF compared with the other two configurations (bPLIF: 573.1 mm$^2$, uPLIF 286.5 mm$^2$, TLIF 341.4 mm$^2$).

Several studies have compared PLIF and TLIF without showing differences in fusion rates between uPLIF and TLIF with posterior instrumentation [16,17] and bPLIF and TLIF with posterior instrumentation [18−21]. However, differences were noted when considering the subsidence rates from clinical studies: The mean subsidence rate for bPLIF is 15.8% (with values ranging from 10% to 65.1%) [5,22−24], whereas the mean subsidence rate for TLIF is approximately 25.3% (with values ranging from 0% to 51.2%) [5,23,25−36], indicating a higher probability of "failure" with TLIF than with bPLIF, highlighting the benefit of a larger contact surface. No clinical studies have compared the outcomes and therefore the fusion rates of stand-alone PLIF and TLIF cages. However, finite element analyses have shown that residual spinal motion may affect fusion rates [37].

Combining the force distribution observations with and without instrumentation, it is possible to make a rough estimate of how much force is transmitted by the rods and how much by the biological tissue (see the Methodology for a detailed explanation). This estimate suggests that, depending on the cage configuration, the human tissues, that is, the annulus and probably to a lesser extent the facet joints, absorb 12%−23% (uPLIF: 16%, bPLIF: 12%, TLIF: 23%) of the axial compressive force (Fig. 6). The dorsal rods, including the screws, absorb 34%−44% (uPLIF: 44%, bPLIF: 38%, TLIF: 34%) of the force. It is interesting to

note that in the uPLIF configuration, the dorsal construct (rods and screws) absorbs approximately 6% more force than in the bPLIF configuration and approximately 10% more than in the TLIF configuration. Therefore, we analysed the axial compressive stiffness data from an older study in our laboratory [38] and found that the stiffness of the construct in the uPLIF configuration is only about half that of the other two configurations. Since screws and rods always have approximately the same stiffness, the lower stiffness can only be due to the fact that the ventral column is less stiff in the uPLIF configuration and therefore the dorsal construct has to bear a greater proportion of the spinal load.

Beside the clinical benefits of intervertebral cages such as the potential to restore the intervertebral height and to aid in restoring sagittal and coronal alignment, the following biomechanical benefits from using intervertebral cages in combination with posterior instrumentation can be assumed: As a result of the increased stiffness of the intervertebral space, a larger proportion of the compressive load is shifted from the screw-rod construct to the intervertebral space, thereby relieving the posterior instrumentation (Fig. 7).

In conclusion, the use of a cage reduces the force on the rods by approximately 29-38% and should therefore reduce the risk of implant failure (Fig. 7). In addition, the reduced load at the bone-screw interface should also minimize the risk of screw loosening, which is one of the major complications of fusion surgery [39]. This biomechanical assumption is supported by a recently published study by Kim et al. [40] who investigated the effect of TLIF on early pedicle screw loosening. Compared to patients who underwent posterolateral fusion, insertion of a TLIF had a protective effect: the rate of early screw loosening was reduced by approximately 60% compared with patients who did not receive a cage.

In addition to the clinical importance, the force applied to a cage is of particular importance to medical device manufacturers. While in the past cages were made of solid material, where material failure was very unlikely, more and more manufacturers are moving to expandable cages. These are designed to minimize the surgical approach, thereby reducing the risk of iatrogenic nerve injury and morbidity [41,42]. However, the fine mechanisms used in expandable cages can usually only withstand a fraction of the ultimate load of a bulky cage. To prevent mechanical failure, current cages are designed to withstand very high loads - a performance goal that is almost impossible to achieve with expandable cages. Given the results of the present study that a maximum of 50% of the forces acting on the spine are transmitted to the cage, expandable cages must at least withstand extreme physiological loads in order to prevent failure. Cage manufacturers could use the sizing data from this study as a guide for their specifications. For example, an average spinal force of 1000N [9,10] could be used to determine endurance test values, with an average of 44% of the external force applied to the cage in the TLIF situation equating to 440N. The average preload of 317N (median TLIF force) would have to be added to this value, giving a total load of 757N. If the same calculation were performed for PLIF cages, the anterior-posterior force distribution would have to be taken into account, as well as the fact that the load is not symmetrical (Appendix 2, Fig. 5). In addition, for expandable cages, it is important to note that the maximum cage expansion may result in significantly higher preloads than in this study, therefore the use of a safety factor should be considered.

This biomechanical in vitro study has several limitations. First, the isolated axial compressive force acting on a vertebral body segment is a simplified loading scenario compared with in-vivo. However, knowing that the axial compression component is the primary load in all loading cases, this is a suitable scenario for the investigation. Second, the minimum height of the cage was 9 mm due to the two embedded load cells. This resulted in the cages possibly being inserted slightly


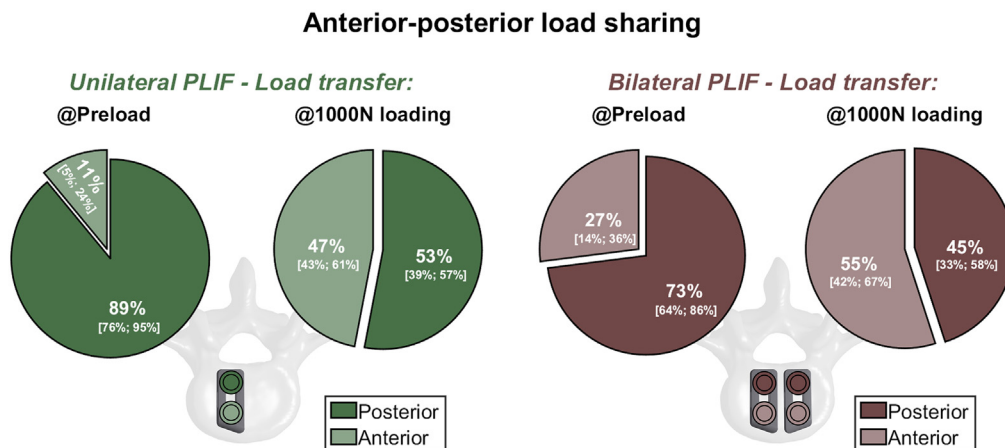
**Anterior-posterior load sharing**

Fig. 5. Relative load distribution in relation to the PLIF site (anterior/posterior) at preload and maximum load with posterior instrumentation. The depicted values indicate the median [25th percentile; 75th percentile].

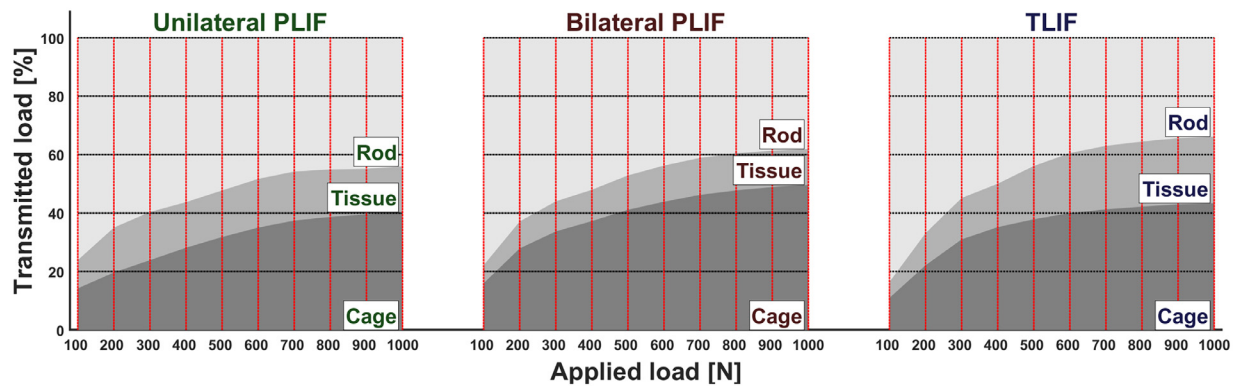## Estimated load sharing
### between cage, tissue, and rod



Fig. 6. Estimated load sharing between cage, tissue (annulus, facet joints), and rod.

more saturated in some cases than in others. However, prior to biomechanical testing, CT scans were obtained to determine the height of the intervertebral disc spaces and to exclude segments that did not meet the minimum height of 9mm. This should have prevented iatrogenic injuries to the endplates as much as possible. Third, although the cages were the same shape as commercially available PLIF and TLIF cages, the surgical approach may have been slightly larger than required in vivo because of the difficulty of inserting the cages with the cables. As the aim of the present study was to quantify

the force acting on the cages under axial compression force with and without posterior instrumentation, the surgical approach is likely to play only a negligible role.

## Conclusion

Without posterior instrumentation, the intervertebral cages absorb more than 50% of the axial load and the load distribution is largely independent of the loading amplitude. With posterior instrumentation, the external load acting on
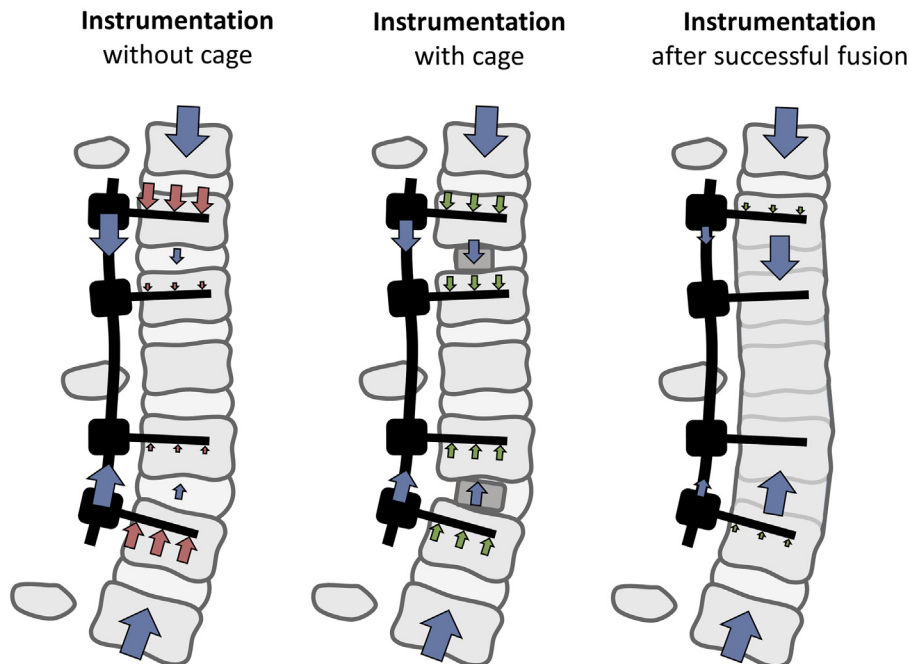


Fig. 7. Illustrations of the axial compression force/force flow on the spine without cage, with cage and after successful bony fusion (from left to right). In instrumentation without a cage, the majority of the load is applied to the top and bottom screws and rods, with only a small fraction is transmitted across the disc space to the subsequent screws. Cage instrumentation allows some compression force to be transmitted through the cage to the screws below, better distributing and reducing the total force on pedicle screws and rods. Successful bony fusion further enhances the effect of force transfer.

the cages is significantly lower and the load distribution becomes load amplitude dependent, with a higher proportion of the load transferred by the cages at high loads. The bPLIF cages tend to absorb more force than the other two cage configurations.

## Declaration of Competing Interest

MF reports being a Consultant for Incremed (Balgrist University Startup), Zimmer Biomet, Medacta, and 25 Segments (Balgrist Startup). All the other authors report no conflicts of interest.

## Authors contributions

AKC: data collection, design of the study, results interpretation, manuscript writing and editing; FC: conception, manuscript editing; MS: technical support, cage design, data collection; SB: conception, manuscript editing; MRF: data analysis and manuscript editing; PS: data collection; MF: conception, manuscript editing; JW: conception, design of the study, results interpretation and manuscript editing

## Availability of data and material

None.

## Ethics approval

Kantonale Ethikkommission Zurich had given the approval for the study. (Basec No. KEK-ZH-Nr. 2022-00104).

## Supplementary materials

Supplementary material associated with this article can be found in the online version at https://doi.org/10.1016/j.spinee.2023.10.017.

## References

[1] Cole CD, McCall TD, Schmidt MH, Dailey AT. Comparison of low back fusion techniques: transforaminal lumbar interbody fusion (TLIF) or posterior lumbar interbody fusion (PLIF) approaches. Curr Rev Musculoskelet Med 2009;2:118–26. https://doi.org/10.1007/s12178-009-9053-8.

[2] Mobbs RJ, Phan K, Malham G, Seex K, Rao PJ. Lumbar interbody fusion: techniques, indications and comparison of interbody fusion options including PLIF, TLIF, MI-TLIF, OLIF/ATP, LLIF and ALIF. J Spine Surg 2015;1:2–18. https://doi.org/10.3978/j.issn.2414-469x.2015.10.05.

[3] Brantigan JW, Steffee AD. A carbon fiber implant to aid interbody lumbar fusion. Spine 1993;18:2106–17. https://doi.org/10.1097/00007632-199310001-00030.

[4] Makanji H, Schoenfeld AJ, Bhalla A, Bono CM. Critical analysis of trends in lumbar fusion for degenerative disorders revisited: influence of technique on fusion rate and clinical outcomes. Eur Spine J 2018;27:1868–76. https://doi.org/10.1007/s00586-018-5544-x.

[5] Amorim-Barbosa T, Pereira C, Catelas D, Rodrigues C, Costa P, Rodrigues-Pinto R, et al. Risk factors for cage subsidence and clinical outcomes after transforaminal and posterior lumbar interbody fusion. European J Orthop Surg Traumatol 2022;32:1291–9. https://doi.org/10.1007/s00590-021-03103-z.

[6] Blumenthal SL, Ohnmeiss DD. NASS. Intervertebral cages for degenerative spinal diseases. Spine J 2003;3:301–9. https://doi.org/10.1016/s1529-9430(03)00004-4.

[7] Evans JH. Biomechanics of lumbar fusion. Clin Orthop Relat Res 1985;193:38–46. https://doi.org/10.1097/00003086-198503000-00005.

[8] Schmoelz W, Keiler A. Intervertebral cages from a biomechanical view. Orthopade 2015;44:132–7. https://doi.org/10.1007/s00132-014-3071-y.

[9] Jost B, Cripton PA, Lund T, Oxland TR, Lippuner K, Jaeger P, et al. Compressive strength of interbody cages in the lumbar spine: the effect of cage shape, posterior instrumentation and bone density. Eur Spine J 1998;7:132–41. https://doi.org/10.1007/s005860050043.

[10] Wilke H, Neef P, Caimi M, Hoogland T, Claes LE. New in vivo measurements of pressures in the intervertebral disc in daily life. Spine 1999;24:755–62. https://doi.org/10.1097/00007632-199904150-00005.

[11] Rastegar S, Arnoux P-J, Wang X, Aubin C-É. Biomechanical analysis of segmental lumbar lordosis and risk of cage subsidence with different cage heights and alternative placements in transforaminal lumbar interbody fusion. Comput Methods Biomech Biomed Engin 2020;23:456–66. https://doi.org/10.1080/10255842.2020.1737027.

[12] Du L, Sun X, Zhou T, Li Y, Chen C, Zhao C, et al. The role of cage height on the flexibility and load sharing of lumbar spine after lumbar interbody fusion with unilateral and bilateral instrumentation: a biomechanical study. BMC Musculoskelet Disord 2017;18:474. https://doi.org/10.1186/s12891-017-1845-1.

[13] Cornaz F, Fasser M-R, Spirig JM, Snedeker JG, Farshad M, Widmer J. 3D printed clamps improve spine specimen fixation in biomechanical testing. J Biomech 2019;98:109467. https://doi.org/10.1016/j.jbiomech.2019.109467.

[14] Cornaz F, Burkhard M, Fasser M-R, Spirig JM, Snedeker JG, Farshad M, et al. 3D printed clamps for fixation of spinal segments in biomechanical testing. J Biomech 2021;125:110577. https://doi.org/10.1016/j.jbiomech.2021.110577.

[15] Committee F. Test methods for intervertebral body fusion devices 2014. https://doi.org/10.1520/f2077-14.

[16] Humphreys SC, Hodges SD, Patwardhan AG, Eck JC, Murphy RB, Covington LA. Comparison of posterior and transforaminal approaches to lumbar interbody fusion. Spine 2001;26:567–71. https://doi.org/10.1097/00007632-200103010-00023.

[17] Audat Z, Moutasem O, Yousef K, Mohammad B. Comparison of clinical and radiological results of posterolateral fusion, posterior lumbar interbody fusion and transforaminal lumbar interbody fusion techniques in the treatment of degenerative lumbar spine. Singapore Med J 2012;53:183–7.

[18] Mehta VA, McGirt MJ, Ambrossi GLG, Parker SL, Sciubba DM, Bydon A, et al. Trans-foraminal versus posterior lumbar interbody fusion: comparison of surgical morbidity. Neurol Res 2011;33:38–42. https://doi.org/10.1179/016164110×12681290831289.

[19] SakebP N, Ahsan K. Comparison of the early results of transforaminal lumbar interbody fusion and posterior lumbar interbody fusion in symptomatic lumbar instability. Indian J Orthop 2013;47:255–63. https://doi.org/10.4103/0019-5413.111484.

[20] Zhang Q, Yuan Z, Zhou M, Liu H, Xu Y, Ren Y. A comparison of posterior lumbar interbody fusion and transforaminal lumbar interbody fusion: a literature review and meta-analysis. BMC Musculoskelet Disord 2014;15:367. https://doi.org/10.1186/1471-2474-15-367.

[21] Rezk EMA, Elkholy AR, Shamhoot EA. Transforaminal lumbar interbody fusion (TLIF) versus posterior lumbar interbody fusion (PLIF) in the treatment of single-level lumbar spondylolisthesis. Egypt J Neurosurg 2019;34:26. https://doi.org/10.1186/s41984-019-0052-9.

[22] Oh KW, Lee JH, Lee J-H, Lee D-Y, Shim HJ. The correlation between cage subsidence, bone mineral density, and clinical results in posterior lumbar interbody fusion. Clin Spine Surg 2017;30:E683–9. https://doi.org/10.1097/bsd.0000000000000315.

[23] Lee N, Kim KN, Yi S, Ha Y, Shin DA, Yoon DH, et al. Comparison of outcomes of anterior, posterior, and transforaminal lumbar interbody fusion surgery at a single lumbar level with degenerative spinal disease. World Neurosurg 2017;101:216–26. https://doi.org/10.1016/j.wneu.2017.01.114.

[24] Suzuki T, Abe E, Miyakoshi N, Murai H, Kobayashi T, Abe T, et al. Posterior-approach vertebral replacement with rectangular parallelepiped cages (PAVREC) for the treatment of osteoporotic vertebral collapse with neurological deficits. J Spinal Disord Techniques 2013;26:E170–6. https://doi.org/10.1097/bsd.0b013e318286fc18.

[25] Zhou Q, Chen X, Xu L, Li S, Du C, Sun X, et al. Does vertebral end plate morphology affect cage subsidence after transforaminal lumbar interbody fusion? World Neurosurg 2019;130:e694–701. https://doi.org/10.1016/j.wneu.2019.06.195.

[26] Park M-K, Kim K-T, Bang W-S, Cho D-C, Sung J-K, Lee Y-S, et al. Risk factors for cage migration and cage retropulsion following transforaminal lumbar interbody fusion. Spine J 2019;19:437–47. https://doi.org/10.1016/j.spinee.2018.08.007.

[27] Mun HY, Ko MJ, Kim YB, Park SW. Usefulness of oblique lateral interbody fusion at L5−S1 level compared to transforaminal lumbar interbody fusion. J Korean Neurosurg S 2019;63:723–9. https://doi.org/10.3340/jkns.2018.0215.

[28] Kim MC, Chung HT, Cho JL, Kim DJ, Chung NS. Subsidence of polyetheretherketone cage after minimally invasive transforaminal lumbar interbody fusion. J Spinal Disord Techniques 2013;26:87–92. https://doi.org/10.1097/bsd.0b013e318237b9b1.

[29] Isaacs RE, Sembrano JN, Tohmeh AG, Group SDS. Two-year comparative outcomes of MIS Lateral and MIS transforaminal interbody fusion in the treatment of degenerative spondylolisthesis. Spine 2016;41:S133–44. https://doi.org/10.1097/brs.0000000000001472.

[30] Choi WS, Kim JS, Ryu KS, Hur JW, Seong JH. Minimally invasive transforaminal lumbar interbody fusion at L5-S1 through a unilateral approach: technical feasibility and outcomes. Biomed Res Int 2016;2016:2518394. https://doi.org/10.1155/2016/2518394.

[31] Kuang L, Wang B, Lü G. transforaminal lumbar interbody fusion versus mini-open anterior lumbar interbody fusion with oblique self-anchored stand-alone cages for the treatment of lumbar disc herniation. Spine 2017;42:E1259–65. https://doi.org/10.1097/brs.0000000000002145.

[32] Lin GX, Quillo-Olvera J, Jo HJ, Lee HJ, Covarrubias-Rosas CA, Jin C, et al. Minimally invasive transforaminal lumbar interbody fusion: a comparison study based on end plate subsidence and cystic change in individuals older and younger than 65 years. World Neurosurg 2017;106:174–84. https://doi.org/10.1016/j.wneu.2017.06.136.

[33] Choi WS, Kim JS, Hur JW, Seong JH. Minimally invasive transforaminal lumbar interbody fusion using banana-shaped and straight cages: radiological and clinical results from a prospective randomized clinical trial. Neurosurgery 2017;82:289–98. https://doi.org/10.1093/neuros/nyx212.

[34] Pereira C, Silva PS, Cunha M, Vaz R, Pereira P. How does minimally invasive transforaminal lumbar interbody fusion influence lumbar radiologic parameters? World Neurosurg 2018;116:e895–902. https://doi.org/10.1016/j.wneu.2018.05.125.

[35] Ko MJ, Park SW, Kim YB. Correction of spondylolisthesis by lateral lumbar interbody fusion compared with transforaminal lumbar interbody fusion at L4−5. J Korean Neurosurg Soc 2019;62:422–31. https://doi.org/10.3340/jkns.2018.0143.

[36] Zhao Y, Jia J, Liu W, Chen X, Mai R, Tian Y, et al. Influence of contoured versus straight rod on clinical outcomes and sagittal parameters in minimally invasive transforaminal lumbar interbody fusion (MIS-TLIF) at L4/5 level-more than 5 years follow-up. J Orthop Sci 2020;25:89–95. https://doi.org/10.1016/j.jos.2019.03.008.

[37] Calvo-Echenique A, Cegoñino J, del Palomar AP. Is there any advantage of using stand-alone cages? A numerical approach. Biomed Eng Online 2019;18:63. https://doi.org/10.1186/s12938-019-0684-8.

[38] Burkhard MD, Spirig JM, Wanivenhaus F, Cornaz F, Fasser M-R, Widmer J, et al. Residual motion of different posterior instrumentation and interbody fusion constructs. Eur Spine J 2023;32:1411–20. https://doi.org/10.1007/s00586-023-07597-5.

[39] Marie-Hardy L, Pascal-Moussellard H, Barnaba A, Bonaccorsi R, Scemama C. Screw loosening in posterior spine fusion: prevalence and risk factors. Global Spine J 2020;10:598–602. https://doi.org/10.1177/2192568219864341.

[40] Kim DH, Hwang RW, Lee G-H, Joshi R, Baker KC, Arnold P, et al. Comparing rates of early pedicle screw loosening in posterolateral lumbar fusion with and without transforaminal lumbar interbody fusion. Spine J 2020;20:1438–45. https://doi.org/10.1016/j.spinee.2020.04.021.

[41] Abbushi A, Čabraja M, Thomale U-W, Woiciechowsky C, Kroppenstedt SN. The influence of cage positioning and cage type on cage migration and fusion rates in patients with monosegmental posterior lumbar interbody fusion and posterior fixation. Eur Spine J 2009;18:1621. https://doi.org/10.1007/s00586-009-1036-3.

[42] Bhatia NN, Lee KH, Bui CNH, Luna M, Wahba GM, Lee TQ. Biomechanical evaluation of an expandable cage in single-segment posterior lumbar interbody fusion. Spine 2012;37:E79–85. https://doi.org/10.1097/brs.0b013e3182226ba6.